FINITE-ELEMENT ANALYSIS OF FUNCTIONALLY GRADED THICK CYLINDER UNDER PRESSURE AND ROTATION

Minor Project

Submitted by

Ayush Srivastav (181116002)
Disha Murali (181116004)

In partial fulfillment of the requirements
For the award of the degree of

BACHELOR OF TECHNOLOGY
in
MECHANICAL ENGINEERING

Under the guidance of

Dr. Vinod Yadav

Department of Mechanical Engineering
Maulana Azad National Institute of Technology Bhopal
Madhya Pradesh – 462003, India

मौलाना आज़ाद राष्ट्रीय प्रौद्योगिकी संस्थान भोपाल 462003 (म.प्र.) भारत
(मानव संसाधन मंत्रालय, भारत सरकार के अधीन राष्ट्रीय महत्व का संस्थान)
Maulana Azad National Institute of Technology Bhopal
Madhya Pradesh – 462003, India
(An Institute of National Importance, Govt. of India)

CERTIFICATE

This is to certify that this report entitled, "**Finite-Element Analysis of Functionally Graded Thick Cylinder under Pressure and Rotation**" submitted by **Ayush Srivastav (181116002)** and **Disha Murali (181116004)** in partial fulfilment of the requirement for the award of Bachelor of Technology Degree in Mechanical Engineering at Maulana Azad National Institute of Technology, Bhopal is a record of bona fide work carried out by them during academic session January 2021 to April 2021, in the Department of Mechanical Engineering at Maulana Azad National Institute of Technology, Bhopal under the supervision of Dr. Vinod Yadav, Assistant Professor in the Department of Mechanical Engineering, Maulana Azad National Institute of Technology, Bhopal. This work has not been submitted to any other university or institute for the award of any other degree or diploma.

Date: 10-04-2021

Dr. Vinod Yadav
Assistant Professor
Department of Mechanical Engineering
Maulana Azad National Institute of Technology, Bhopal
Madhya Pradesh – 462003, India

मौलाना आज़ाद राष्ट्रीय प्रौद्योगिकी संस्थान भोपाल 462003 (म.प्र.) भारत
(मानव संसाधन मंत्रालय, भारत सरकार के अधीन राष्ट्रीय महत्व का संस्थान)
Maulana Azad National Institute of Technology Bhopal
Madhya Pradesh – 462003, India
(An Institute of National Importance, Govt. of India)

ACKNOWLEDGEMENT

We would like to express our sincere gratitude to our project guide Dr. Vinod Yadav, Assistant Professor in the Department of Mechanical Engineering at Maulana Azad National Institute of Technology, Bhopal for his continuous guidance and suggestions.

We express our sincere thanks to the Department of Mechanical Engineering at Maulana Azad National Institute of Technology, Bhopal for providing the technological support for our project. Lastly, we extend our heartiest gratitude to all the faculty members of Maulana Azad National Institute of Technology, Bhopal for their encouragement.

Date: 10-04-2021

Ayush 12/04/2021
Ayush Srivastav
181116002
Pre-final year
B.Tech Mechanical Engineering

ISHA 12-04-21
Disha Murali
181116004
Pre-final year
B.Tech Mechanical Engineering

Abstract

The purpose of this study is to investigate the effects of material inhomogeneity on thick cylinders under rotation with uniform internal and external pressure. The work is motivated by the recent research activity on functionally graded materials (FGMs), i.e., materials with spatially varying properties tailored to satisfy particular engineering applications. In this report, the elastic analysis for a thick cylinder made of isotropic material and thick cylinders made of FGMs is carried out using Finite-Element Method (FEM). The property of FGMs is assumed to be of exponential function form with Young's modulus depending on the radial coordinate only, and constant Poisson's ratio. It is shown that the stress response of the inhomogeneous cylinder is significantly different from that of the homogeneous cylinder. Stress distributions along the radial and circumferential directions are studied, assuming the stress in axial direction to be zero. Results shows that the property of FGMs has a significant influence on the stress distributions – reducing the overall radial stress and completely changing the distribution of circumferential stress as compared to the stress distributions in an isotropic cylinder under same load. Thus, using the exclusively designed functionally graded materials for manufacturing of parts can increase their pressure handling capacity and improve their functionality.

Keywords: thick cylinder, isotropic material, functionally graded materials, analytical modelling, finite element analysis.

Content

Notations

a	inner radius of the cylinder
b	outer radius of the cylinder
σ_r	radial stress component
σ_θ	circumferential stress component
σ_z	axial stress component
ε_r	radial strain
ε_θ	circumferential strain
ε_z	axial strain
u_r	radial displacement
ν	Poisson's ratio
E	modulus of elasticity
E_o	constant of modulus of elasticity
C_1, C_2	constants of homogeneous diff. equation
ρ	density of the material
ρ_o	constant for density of the material
ω	angular velocity of the rotation
P_i, P_o	internal and external pressure
$F(r)$	stress function
σ_{yield}	yield stress
β_1, β_2	power law exponent of modulus of elasticity and density

Chapter 1
Introduction and Literature Review

1.1 Introduction

Thick cylindrical shells are common structural elements in many engineering applications, including pressure vessels, submarine hulls, ship hulls, wings and fuselages of airplanes, containment structures of nuclear power plants, pipes, exteriors of rockets, missiles, automobile tires, concrete roofs, chimneys, cooling towers, liquid storage tanks, and many other structures. In order to optimize the weight, mechanical strength, displacement and stress distribution of a shell, one approach is to use shells with functionally graded materials.

Functionally graded materials (FGMs) have continuously varying material composition from one surface to another surface which makes these materials non-homogeneous in terms of both the material properties and microstructures. Usually, a ceramic is used at one surface to resist severe environmental effect, such as high temperature, wear, and corrosion; and a metal is used at the other surface to ensure higher toughness and thermal conductivity. It was first invented in 1984 by Japanese researchers for the core purpose of their aerospace project that required thermal barrier with the outside temperature of 2000 K and inside 1000 K within 10 mm thickness. They are primarily used as coatings and interfacial zones to reduce stresses resulting from the material property mismatch, to improve the surface properties and to provide protection against severe loading, thermal and chemical environments. Aside from the thermal barrier coatings, some of the potential applications of FGMs include their use as interfacial zones to improve the bonding strength and to reduce residual stresses in bonded dissimilar materials and as wear-resistant layers such as gears, cams, ball and roller bearings and machine tools.

In Functionally graded materials, some particular physical properties are changed with the change in dimensions. Such material properties can be described by a function $f(x)$. In case of homogeneous materials this function reduces to a constant.

1.2 Application

Functionally graded materials have been used in many fields such as aerospace, nuclear energy, biology, electromagnetism, optics, energy and other fields through the ingenious combination of inorganic and organic materials such as metals, ceramics and plastics.

1.2.1 Aerospace Field

Functionally graded materials with high temperature resistance, thermal shock resistance, thermal fatigue resistance and corrosion resistance can be applied to heat-resistant surface of space shuttle and aircraft engine parts [1]. Spacecraft engine combustion chamber wall at work, the side need to withstand high temperature and thermal erosion above 2000K, the material has excellent heat and heat insulation properties, while the other side will have low

temperature liquid hydrogen cooling, the material proposed low temperature and high thermal conductivity requirements.

1.2.2 Nuclear Energy Field

The high strength, heat resistance and corrosion resistance of FGM provide a reliable guarantee for the development of next generation nuclear industry. As a high-strength, heat-resistant and shielding material, functionally graded materials show great superiority in the construction materials of nuclear furnaces and inner wall materials of nuclear furnaces, which greatly protects the safety of the nuclear industry [2].

1.2.3 Machine Tool Technology

Cho and Park [3] have investigated the thermo-elastic characteristics of functionally graded lathe cutting tools composed of Cr–Mo steel shank and ceramic tip with a view to exploring its thermo-mechanical superiority. They found that the thermo-mechanical stress concentration was significantly relaxed by adding an FGM layer between the steel shank and the ceramic tip and thus justified the potential of FGMs for high performance metal cutting tools. A.M. Afsar and J. Go [4] have investigated the application of FGMs in a circular disk type cutter or a grinding disk for better performance. Along with the thermal load and inertia force due to rotation of the disk, they accounted for the effect of the incompatible eigen strain developed in the disk due to non-uniform CTE.

1.2.4 Electromagnetic Field

In the electromagnetic field, the FDMs gradient structure has the piezoelectric gradient function and the electromagnetic gradient function, and can be used to make electromagnetic shielding materials, ceramic filters, ultrasonic oscillators, etc. [5]

1.2.5 Energy Sector

FGM are used in energy conversion devices. They also provide thermal barrier and are used as protective coating on turbine blades in gas turbine engine [6]. In the aspect of power generation system, the application of gradient thermoelectric energy conversion material makes the emitter not cracked in the high temperature working environment of 1860°C and greatly reduces the thermal stress of the system. Meanwhile, the application of the heat release substrate at the low temperature electrode of the system also shows high thermal conductivity and radiation exothermic rate [7].

1.2.6 Commercial and Industrial Sector

Other than the above described, FGMs can also be used for Pressure vessels, Fuel tanks, Cutting tool inserts, Laptop cases, Wind turbine blades, Firefighting air bottles, MRI scanner cryogenic tubes, Eyeglass frames, Musical instruments, Drilling motor shaft, X-ray tables, Helmets [8].

1.3 Literature Review

Naki Tutuncu [9], presented a paper in which the stress and displacement solutions are obtained in thick-walled FGM cylinders subjected to internal pressure only. The material is

assumed to be isotropic with exponentially-varying elastic modulus through the thickness as $E = E_0 e^{\beta r}$, and obtained solution in the form of power series using Frobenius method. A work was published by Horgan and Chan [10] where it was noted that increasing the positive exponent of the radial coordinate provided a stress shielding effect whereas decreasing it created stress amplification. Similarly, Tutuncu and Ozturk [11] obtained closed form solutions for cylindrical and spherical vessels with variable elastic properties obeying a simple power law through the wall thickness which resulted in simple Euler–Cauchy equations whose solutions were readily available. Chen and Lin [12] investigated stresses and displacements in FGM cylindrical and spherical pressure vessels based on the assumptions that Poisson's ratio is constant and modulus of elasticity is an exponential function of radius. They discovered that the properties of FGMs have a substantial impact on the stress distribution in the radial direction. Evci and Gülgeç [13] presented an analytical solution of stresses and displacements in a long FGM hollow cylinder subjected to uniform heat generation and internal pressure. The stress analysis shows that for a given range of material parameters, stresses in FGM cylinders are significantly lower than in homogeneous cylinders. The findings of the stress analysis are supported by radial displacement analysis in the FGM cylinder.

Many works were published considering the rotating FGM cylinder under various loading conditions. For example, stresses on isotropic rotating thick-walled cylindrical pressure vessels made of FGM are obtained as a function of radial direction by using the theory of elasticity Navier equation by Nejad and Rahimi [14]. J.N. Sharma, D. Sharma and Kumar [15] They calculated thermo-elastic stresses, displacements, and strains in a thin circular rotating functionally graded material (FGM) disc subjected to thermal loads using finite element analysis. In addition, the temperature profiles were modeled using the heat conduction equation. Similarly, for rotating discs in a body-fixed or a space-fixed co-ordinate scheme, Nigh and Olson [16] used the finite element form; and Zafarmand [17] studied two-dimensional functionally graded rotating annular and solid discs with variable thickness using elastic analysis. For the two-dimensional functionally graded disc, axisymmetric conditions are assumed, and the equations are solved using the graded finite element method (GFEM). Zenkour [18] investigated the stress distribution in rotating composite structures of FGM solid discs. Afsar and Go [4] used the finite element approach to investigate the thermoelastic field in a revolving FGM circular disc, taking into account uniform exponential and parabolic temperature variations. Bayat(2009) [19] presented their findings on the study of a revolving disc with variable thickness FGM. The disc is subjected to both mechanical and thermal loads, and the material properties differ according to the power law. Bayat et al. (2011) [20] used a semi-analytical approach to examine the displacement and stress activity of a functionally graded rotating disc of variable thickness. Material properties differ according to power law and Mori Tanaka scheme in radially varying one-dimensional FGM. The fixed boundary condition at the inner surface and the free boundary condition at the outer surface of a disc subjected to centrifugal load was investigated. Rosyid [21] studied a non-homogeneous rotating disc with arbitrarily variable thickness using finite element analysis. For volume fraction distributions, three types of grading laws are considered: power law, sigmoid law, and exponential distribution law. In a recent work, Dewangan, Sodhi and Tiwari [22] investigated rotating thick discs with clamped free boundary conditions made of two-

dimensional FGM. By using element-based material grading, the material properties of the discs are graded in both the radial and axial directions according to power law distribution.

1.4 Inference from Literature Review

Total stresses due to centrifugal load plays a very important role on the strength and safety of many mechanical components such as gears, grinding cutters, rollers for hot working. Thus, optimization of total stresses and displacement fields is important. A number of researches have been conducted analytically as well as through FEM for a thick rotating disk of FGM for the above-described scenario. In most of the literatures reviewed, the pressure is assumed to be acting on the internal surface while rotating; or rotation is not at all taken into account when the pressure is acting on both internal and external surfaces. Thus, there is need to investigate the stress distribution for a rotating FGM cylinder subjected to pressure acting on both the surfaces.

1.5 Objective of Present work

Based on the literature review, the focus of our present work will be

- To perform Finite-Element Analysis (FEA) of a thick functionally graded cylinder under pressure and rotation.
- To compare the radial and hoop stresses in a functionally graded cylinder with that of an isotropic cylinder of same dimensions under same load conditions.

1.6 Organization of the report

- First chapter presents an introduction, a brief literature review and the objectives of our present work.
- Second chapter explains the behavior of a thick isotropic and FGM cylinder under pressure and rotation using Analytical Modelling.
- Third chapter, presents the procedure for Finite-Element Modeling of both the isotopic and FGM cylinder under internal pressure, external pressure and rotation.
- Fourth chapter, discusses the results of the parametric study in detail.
- Fifth chapter, establishes the conclusions of our study and explains the scope of future work.
- Appendix contains the MATLAB codes used for plotting the graphs for isotropic and FGM cylinders presented in this report.

Chapter 2
Analytical Modelling

In this chapter, analytical modeling of a thick cylinder is presented. The geometry of hollow cylinder is described using the cylindrical coordinate system with coordinates x, θ and r denoting the axial, circumferential and radial coordinates, respectively. A long axi-symmetric cylinder with inner radius ‘‘a” and outer radius ‘‘b” is investigated. The internal and external pressures applied to the hollow cylinder are also axi-symmetric. Since the applied loads and material properties are independent of θ, mechanical solutions are assumed to be axi-symmetric.

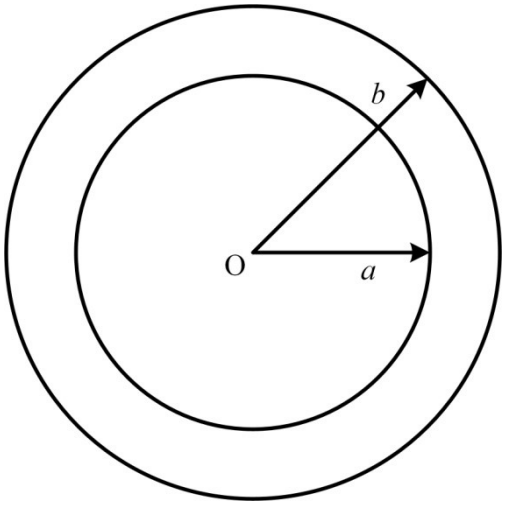

Figure 1. A long axi- symmetric cylinder

2.1 Elastic analysis of a stationary isotropic cylinder

Stress and displacement analysis of a cylinder which is free to expand in the axial direction can be treated as generalized plane strain problem. In the absence of the body forces, equations of equilibrium in cylindrical coordinates reduces to [23]

$$\frac{\partial \sigma_r}{\partial r} + \frac{\sigma_r + \sigma_\theta}{r} = 0 \quad (1)$$

where σ_r is the radial stress component, σ_θ is the circumferential stress component and r the radial coordinate? The generalized Hooke’s law can be used in the purely elastic body to express the relationship between the stresses and strains as follows [23]

$$\varepsilon_r = \frac{1}{E}(\sigma_r - \nu\sigma_\theta) \quad (2)$$

$$\varepsilon_\theta = \frac{1}{E}(\sigma_\theta - \nu\sigma_r) \quad (3)$$

where E is the Young’s modulus and ν is Poisson ratio.

The radial and circumferential strain components are related to the radial displacement u_r by

$$\varepsilon_r = \frac{du_r}{dr} \quad (4)$$

$$\varepsilon_\theta = \frac{u_r}{r} \quad (5)$$

The relation between the radial and circumferential strain components (as given by Eq. (4) and Eq. (5)) introduces a compatibility equation given by [23]

$$\frac{\varepsilon_r-\varepsilon_\theta}{r}-\frac{d\varepsilon_\theta}{dr}=0 \tag{6}$$

Combining equation (2) and (3) into equation (6) we have

$$r\frac{d\sigma_\theta}{dr}-\nu r\frac{d\sigma_r}{dr}+(1+\nu)(\sigma_\theta-\sigma_r)=0 \tag{7}$$

Differentiating equation (1) we have

$$\frac{d\sigma_\theta}{dr}=r\frac{d^2\sigma_r}{dr^2}+2\frac{d\sigma_r}{dr} \tag{8}$$

Combining this with equation (7), we get the governing differential equation as

$$r\frac{d^2\sigma_r}{dr^2}+3\frac{d\sigma_r}{dr}=0 \tag{9}$$

On solving equation (9) we get

$$\sigma_r=C_1+\frac{C_2}{r^2} \tag{10}$$

$$\sigma_\theta=C_1-\frac{C_2}{r^2} \tag{11}$$

Applying boundary conditions,

$$\sigma_r=P_i \qquad \text{at r = a} \tag{12}$$

$$\sigma_\theta=P_o \qquad \text{at r = b}$$

The radial and circumferential stresses are given by

$$\sigma_r=\frac{(P_ia^2-P_ob^2)}{(b^2-a)^2}+\frac{(P_o-P_i)a^2b^2}{(b^2-a^2)r^2} \tag{13}$$

$$\sigma_\theta=\frac{(P_ia^2-P_ob^2)}{(b^2-a)^2}-\frac{(P_o-P_i)a^2b^2}{(b^2-a^2)r^2} \tag{14}$$

2.2 Elastic analysis of a rotating isotropic cylinder

For the case of a rotating cylinder, the equations (2), (3), (4), (5), (6) and (7) remain unchanged, whereas the equilibrium equation (1) is modified as [24]

$$\frac{\partial\sigma_r}{\partial r}+\frac{\sigma_r-\sigma_\theta}{r}+\rho\omega^2r^2=0 \tag{15}$$

where ρ is the density of the material and ω is the angular velocity of the rotation.

From the above modification (equation (15)), the governing differential equation is obtained as

$$r\frac{d^2\sigma_r}{dr^2}+3\frac{d\sigma_r}{dr}=-(3+\nu)\rho\omega^2r^2 \tag{16}$$

On solving equation (15), we get

$$\sigma_r=C_1+\frac{C_2}{r^2}-\frac{(3+\nu)}{8}\rho\omega^2r^2 \tag{17}$$

$$\sigma_r=C_1-\frac{C_2}{r^2}-\left[1-\frac{3(3+\nu)}{8}\right]\rho\omega^2r^2 \tag{18}$$

Applying boundary conditions,

$$\sigma_r=P_i \qquad \text{at r = a}$$

$$\sigma_\theta=P_o \qquad \text{at r = b}$$

The radial and circumferential stresses are found as

$$\sigma_r = \left[\frac{(P_i a^2 - P_o b^2)}{(b^2-a)^2} - \frac{(3+\nu)}{8}\rho\omega^2(b^2-a^2)\right] + \frac{1}{r^2}\left[\frac{(P_o - P_i)a^2b^2}{(b^2-a^2)} - \frac{(3+\nu)}{8}\rho\omega^2 a^2 b^2\right] - \frac{(3+\nu)}{8}\rho\omega^2 r^2 \quad (19)$$

$$\sigma_\theta = \left[\frac{(P_i a^2 - P_o b^2)}{(b^2-a)^2} - \frac{(3+\nu)}{8}\rho\omega^2(b^2-a^2)\right] - \frac{1}{r^2}\left[\frac{(P_o - P_i)a^2b^2}{(b^2-a^2)} - \frac{(3+\nu)}{8}\rho\omega^2 a^2 b^2\right] - \left[1 - \frac{3(3+\nu)}{8}\right]\rho\omega^2 r^2 \quad (20)$$

2.3 Analysis of a stationary FGM Cylinder

In the case of Functionally Graded Material, the equilibrium equation (1) and the compatibility equation (6) remains unchanged.

The equilibrium equation given by Eq. (11) is satisfied if the stress function $F(r)$ is introduced such that

$$\sigma_r = \frac{F(r)}{r} \quad (21)$$

$$\sigma_\theta = \frac{dF(r)}{dr} \quad (22)$$

Assuming that Poisson's ratio remains constant throughout the geometry, the Young's Modulus and yield stresses are assumed as functions of radial coordinates

$$E = E(r) \quad (23)$$

$$\sigma_{yield} = \sigma_{yield}(r) \quad (24)$$

Assuming again the plan strain case we have

$$\varepsilon_z = \frac{1}{E}[\sigma_z - \nu(\sigma_r + \sigma_\theta)] = 0 \quad (25)$$

$$\sigma_z = \nu(\sigma_r + \sigma_\theta) \quad (26)$$

From the above relation, we can arrive at

$$\varepsilon_r = \frac{(1+\nu)}{E}[\sigma_r(1-\nu) - \nu\sigma_\theta] \quad \& \quad \varepsilon_\theta = \frac{(1+\nu)}{E}[\sigma_\theta(1-\nu) - \nu\sigma_r] \quad (27)$$

Substituting the values of ε_r, ε_θ, σ_r, σ_θ from equation (21), (22) and (27) into compatibility equation, we get the governing differential equation as

$$\frac{d^2F}{dr^2} + \frac{1}{r}\frac{dF}{dr} - \frac{F}{r^2} - \left(\frac{dF}{dr} - \frac{\nu}{1-\nu}\frac{F}{r}\right)\frac{1}{E(r)}\frac{dE(r)}{dr} = 0 \quad (28)$$

2.3.1. Power Function

In this model we assume that the Young's Modulus varies as a power function,

$$E(r) = r^\beta \quad (29)$$

where, E_0 is constant for Modulus of elasticity, radius at the point of material definition

β is a constant that controls the behavior of power function.

Substituting the expression for Young's Modulus equation (29) into (28)

$$r^2\frac{d^2F}{dr^2} + (1-\beta)r\frac{dF}{dr} - \left(1 - \frac{\nu\beta}{1-\nu}\right)F = 0 \quad (30)$$

Upon solving the above differential equation which assumes Cauchy-Euler equation we get

$$F(r) = C_1 r^{m_1} + C_2 r^{m_2} \tag{31}$$

$$\sigma_r(r) = \frac{F(r)}{r} = C_1 r^{m_1-1} + C_2 r^{m_2-1} \tag{32}$$

$$\sigma_\theta(r) = \frac{dF(r)}{dr} = C_1 m_1 r^{m_1-1} + C_2 r^{m_2-1} \tag{33}$$

$$\text{where, } m_{1,2} = \frac{-\beta \pm \sqrt{\beta^2 - 4(1-\frac{\nu}{1-\nu})\beta}}{2} \tag{34}$$

Applying the same boundary conditions as in equation (12), we obtain the constants as

$$C_1 = \frac{-P_i + P_o\left(\frac{a}{b}\right)^{m_2-1}}{a^{m_1-1} - a^{m_2-1} b^{m_1-m_2}}$$
$$C_2 = \frac{-P_o}{b^{m_2-1}} + \frac{P_i - P_o\left(\frac{a}{b}\right)^{m_2-1}}{a^{m_1-1} - a^{m_2-1} b^{m_1-m_2}} b^{m_1-m_2} \tag{35}$$

The expression thus obtained for radial and hoop stresses are

$$\sigma_r = \frac{-P_i + P_o\left(\frac{a}{b}\right)^{m_2-1}}{a^{m_1-1} - a^{m_2-1} b^{m_1-m_2}} r^{m_1-1} + \left[\frac{-P_o}{b^{m_2-1}} + \frac{P_i - P_o\left(\frac{a}{b}\right)^{m_2-1}}{a^{m_1-1} - a^{m_2-1} b^{m_1-m_2}} b^{m_1-m_2}\right] r^{m_2-1}$$

$$\sigma_\theta = \frac{-P_i + P_o\left(\frac{a}{b}\right)^{m_2-1}}{a^{m_1-1} - a^{m_2-1} b^{m_1-m_2}} m_1 r^{m_1-1} + \left[\frac{-P_o}{b^{m_2-1}} + \frac{P_i - P_o\left(\frac{a}{b}\right)^{m_2-1}}{a^{m_1-1} - a^{m_2-1} b^{m_1-m_2}} b^{m_1-m_2}\right] m_2 r^{m_2-1} \tag{36}$$

2.3.2. Exponential Function

In this model we assume that the Young's Modulus varies as an exponential function,

$$E(r) = E_0 e^{\left(\frac{\beta(r-a)}{b-a}\right)} \tag{37}$$

where, E_0 is constant for modulus of elasticity, r is the radius at the point of material definition, β is a constant which controls the behavior of exponential function.

Now, substituting the expression for Young's Modulus equation (37) into (28) we get

$$\frac{d^2F}{dr^2} + \left[1 - \frac{\beta r}{(b-a)}\right]\frac{1}{r}\frac{dF}{dr} - \left[1 - \frac{\nu}{(1-\nu)r^2}\frac{\beta}{b-a}\right]F = 0 \tag{38}$$

The solution for the above equation assumes the form

$$F(r) = F_1(r) + cF_2(r) \tag{39}$$

where F_1 and F_2 can be evaluated by the boundary conditions equation (12) using numerical differentiation for which Runge-Kutta Method of order four is used. From the expression (39), the radial and hoop stress distribution is obtained.

2.4 Analysis of a rotating FGM Cylinder

The equilibrium equation in the radial direction, neglecting the body force components, is reduced to a single equation (15)

$$\frac{\partial \sigma_r}{\partial r} + \frac{\sigma_r - \sigma_\theta}{r} + \rho\omega^2 r = 0$$

where ρ is the density of the material and ω is the angular velocity of the rotation.
The governing differential equation is obtained in the form of Navier's equation as

$$\frac{d^2u_r}{dr^2} + \left(\frac{1}{E}\frac{dE}{dr} + \frac{1}{r}\right)\frac{du_r}{dr} + \left(\frac{n}{Er}\frac{dE}{dr} - \frac{1}{r^2}\right)u_r = -\frac{\rho\omega^2}{C_{11}E}r \quad (40)$$

where, $C_{11} = \frac{(1-\nu)}{(1+\nu)(1-2\nu)}$, $C_{12} = \frac{\nu}{(1+\nu)(1-2\nu)}$ and $n = \frac{\nu}{(1-\nu)}$.

2.4.1. Power function

The modulus of elasticity and density through the wall thickness are assumed to vary as follows:

$$E = E_o r^{\beta_1} \text{ and } \rho = \rho_o r^{\beta_2} \quad (41)$$

Using equation (40) and (41), the governing differential equation becomes

$$r^2\frac{d^2u_r}{dr^2} + (1+\beta_1)r\frac{du_r}{dr} + (n\beta_1 - 1)u_r = -\frac{\rho_i\omega^2 a^{\beta_1-\beta_2}}{E_o C_{11}} r^{\beta_2-\beta_1+3} \quad (42)$$

The solution for this differential equation is evaluated analyzed deeply by Nejad and Rahimi [14] which takes the form as

$$u_r(r) = A_1 r^{m_1} + A_2 r^{m_2} + A_3 r^{m_3}$$

where A_1, A_2, A_3, m_1 , m_2 and m_3 are constant determined by solving equation (42).

2.4.2. Exponential function

The modulus of elasticity and density through the wall thickness are assumed to vary as follows:

$$E = E_o r^{\left(\frac{\beta_1(r-a)}{b-a}\right)} \text{ and } \rho = \rho_o r^{\left(\frac{\beta_2(r-a)}{b-a}\right)} \quad (43)$$

Substituting equation (43) into equation (40), we arrive at

$$\frac{d^2u_r}{dr^2} + \left(\frac{\beta_1}{b-a} + \frac{1}{r}\right)\frac{du_r}{dr} + \left(\frac{n}{r}\frac{\beta_1}{b-a} - \frac{1}{r^2}\right)u_r = -\frac{\rho_o\omega^2}{C_{11}E_o} r^{(\beta_2-\beta_1)\left(\frac{r-a}{b-a}\right)} \quad (44)$$

The solution for the above kind of differential equation cannot be determined by direct methods. Thus, the radial displacement can be obtained by numerical differentiation methods, and from that radial and hoop stresses can be evaluated.

Chapter 3
Finite-Element Modelling

In this chapter, the Finite-Element Analysis (FEA) of a thick cylinder is presented. A commercially available FEM software package ABAQUS 6.10 is used to simulate the isotropic and functionally graded thick cylinders under varying pressure loads and rotational velocity.

3.1 Geometric Parameter

According to [25], the ratio of internal radius (r_i) to thickness (t) is less than 10 (i.e., $\frac{r_i}{t} < 10$) for thick-walled cylindrical pressure vessels. Hence, the dimensions of the cylinder are assumed as follows, internal radius (r_i) = 0.3 m, external radius (r_e) = 0.5 m and height (h) = 1 m for the Finite Element Modelling (FEM).

As per the axisymmetric assumption the cylinder can be reduced to a rectangle with the correct geometry and appropriate boundary conditions for FEM. Create an axisymmetric deformable shell part with the geometry as shown in Figure 2.

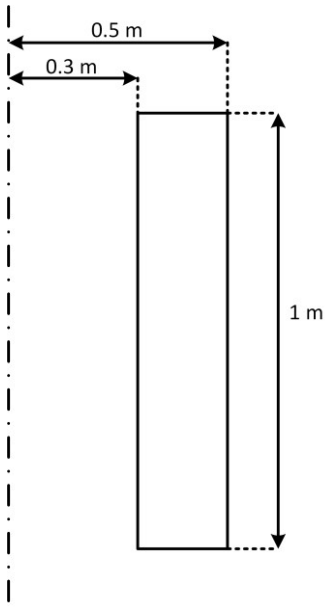

Figure 2. Geometry of the part created for FEA

3.2 Material Properties

Material definition is the only distinction between the FEM of the isotropic cylinder and the cylinder made of Functionally Graded Material (FGM).

3.2.1 Isotopic Cylinder

Isotropic materials have identical material properties in all directions at every given point over the volume of the system.

The isotropic cylinder is assumed to be made up of AISI 1045 Medium Carbon Steel. The material properties used for the FEA are given in Table 1.

Table 1. Material properties of AISI 1045 Medium Carbon Steel

Properties	**Symbol**	**Value**	**Units**
Density	ρ	7870	Kg/m^3
Modulus of Elasticity	E	200	GPa
Poisson's Ratio	ν	0.29	(Unitless quantity)

3.2.2 FGM Cylinder

Functionally Graded Materials are characterized by the gradual variation in composition and structure over the volume of the system, resulting in corresponding changes in the material properties. These materials are designed for specific function and applications.

The FGM cylinder is assumed to be made up of functionally graded material with the base properties of AISI 1045 Medium Carbon Steel varying according to one of the functions listed below in the FEA.

3.2.2.1 Power Function

Assuming the FGM varies according to the power function i.e., the Young's Modulus follows the power function and the Poisson's ratio is constant.

$$E(r) = E_0 r^{\beta}$$

where, E_0 = Modulus of elasticity of AISI 1045 Medium Carbon Steel
r = radius at the point of material definition
β = constant (controls the behavior of power function)

Microsoft Excel is used to calculate E(r) at discrete values of r varying from r_i = 0.3 m to r_e = 0.5 m for β = 0.1667 (selected to keep the calculated values of E in a sizable range) as shown in Table 2.

Table 2. Material Properties of FGM defined by *power function*

Modulus of Elasticity, *E* *(in N/mm^2)*	**Poisson's Ratio, *ν***	**Radius, *r*** (in mm)
517468.0474	0.29	300
523064.1944	0.29	320
528376.08	0.29	340
533433.6551	0.29	360
538262.2574	0.29	380
542883.5233	0.29	400
547316.0837	0.29	420
551576.1025	0.29	440
555677.699	0.29	460
559633.2829	0.29	480
563453.8228	0.29	500

3.2.2.2 Exponential Function

Assuming the FGM varies according to the exponential function i.e., the Young's Modulus follows the exponential function and the Poisson's ratio is constant.

$$E(r) = E_0 e^{\left(\frac{\beta(r-a)}{b-a}\right)}$$

where, E_0 = Modulus of elasticity of AISI 1045 Medium Carbon Steel
r = radius at the point of material definition
β = constant (controls the behavior of power function)
a = undeformed internal radius of cylinder
b = undeformed external radius of cylinder

Microsoft Excel is used to calculate E(r) at discrete values of r varying from r_i = 0.3 m to r_e = 0.5 m for β = 1 (selected to keep the calculated values of E in a sizable range) as shown in Table 3.

Table 3. Material Properties of FGM defined by *exponential function*

Modulus of Elasticity, *E* *(in N/mm^2)*	**Poisson's Ratio, *ν***	**Radius, *r*** (in mm)
200000	0.29	300
221034.1836	0.29	320
244280.5516	0.29	340
269971.7615	0.29	360
298364.9395	0.29	380
329744.2541	0.29	400
364423.7601	0.29	420
402750.5415	0.29	440
445108.1857	0.29	460
491920.6222	0.29	480
543656.3657	0.29	500

These tabulated values are input into ABAQUS as the definition of the functionally graded material's elasticity using an Analytical Field created along the x-axis. This virtually divides the rectangle into 11 separate sections, each with a different material property (*i.e.,* Modulus of Elasticity, E) thus, defining the functionally graded cylinder discretely.

3.3 Load and boundary conditions

Three loads are applied on the rectangular geometry for the FEA of rotating thick cylindrical pressure vessels – an internal pressure (p_i), an external pressure (p_e) and a rotating body force of angular velocity (ω).

The boundary condition required to define the FEM is a YSYMM (U2 = UR1 = UR3 = 0) on the bottom edge of the rectangle as shown in Figure 3 to restrict the change in y-coordinate of the bottom edge.

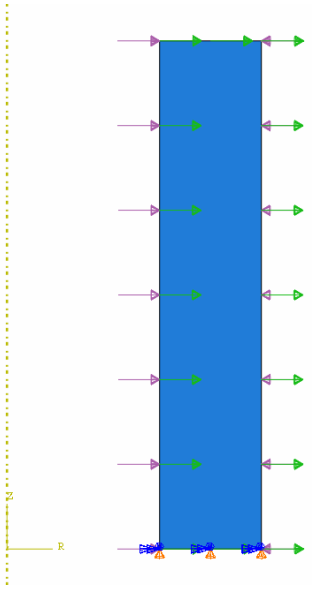

Figure 3. Load (p_i, p_e and ω) and Boundary conditions (Y SYMM)

3.4 Element type and mesh sensitivity

Considering the geometry of the model, a structured quad element shape is selected to mesh the part. A 4-node bilinear axisymmetric quadrilateral (CAX4) element type is selected from the axisymmetric stress family.

Mesh sensitivity analysis for the finite-element model is carried out based on the convergence of minimum radial and hoop values stresses to a stationary value by varying the number divisions of the geometry. The optimum mesh is attained at 67 divisions along the x-axis and 333 divisions along the y-axis, with 22311 elements and 22712 nodes as shown in Figure 4.

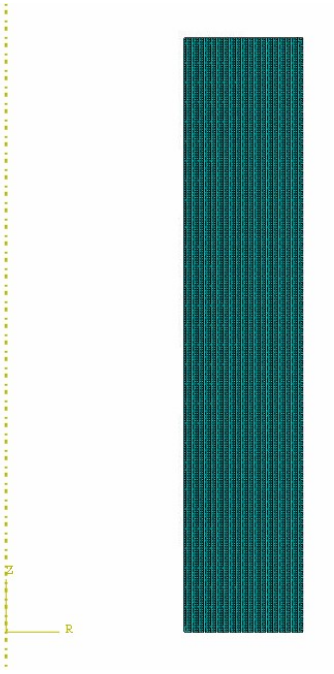

Figure 4. Structured quad CAX4 Mesh

Chapter 4
Results and Discussion

4.1 Varying internal pressure without rotation for isotropic cylinder

The radial and hoop stress distributions in the isotropic thick cylinder at internal pressure, P_i = 5, 15 & 25 MPa and angular velocity, ω = 0 are illustrated in Figure 5 (a) & (b). The results of Analytical Model are validated with the results of FEA as shown in Figure 5.

As depicted in Figure 5(a) the magnitude of radial stress at the deformed inner radius is equal to the applied internal pressure. The radial stress increases exponentially to reach 0 at the deformed outer radius. Figure 5(b) shows the exponential decrease in the hoop stress from the maximum value at the deformed inner radius to the minimum value at the deformed outer radius.

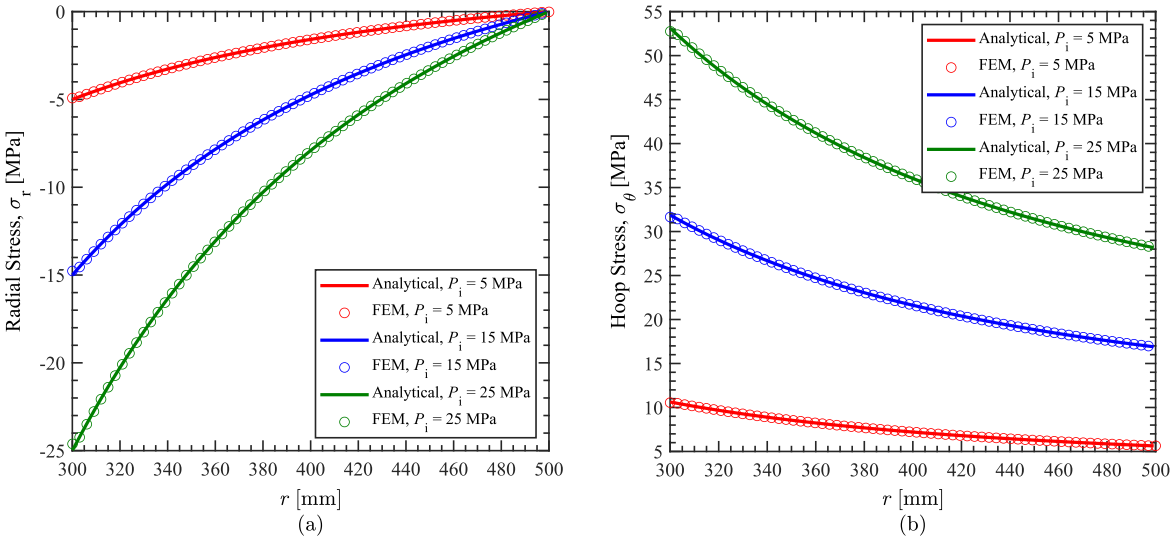

Figure 5. (a) Radial stress distribution (b) hoop stress distribution at internal pressure, P_i = 5, 15 & 25 MPa and angular velocity, ω = 0

4.2 Varying external pressure without rotation for isotropic cylinder

The radial and hoop stress distributions in the isotropic thick cylinder at external pressure, P_e = 1, 5 & 10 MPa and angular velocity, ω = 0 are illustrated in Figure 6 (a) & (b). The results of Analytical Model are validated with the results of FEA as shown in Figure 6.

As depicted in Figure 6(a) the magnitude of radial stress at the deformed inner radius is equal to 0. The radial stress decreases exponentially to reach the applied internal pressure at the deformed outer radius. Figure 6(b) shows the exponential increase in the hoop stress from the minimum value at the deformed inner radius to the maximum value at the deformed outer radius.

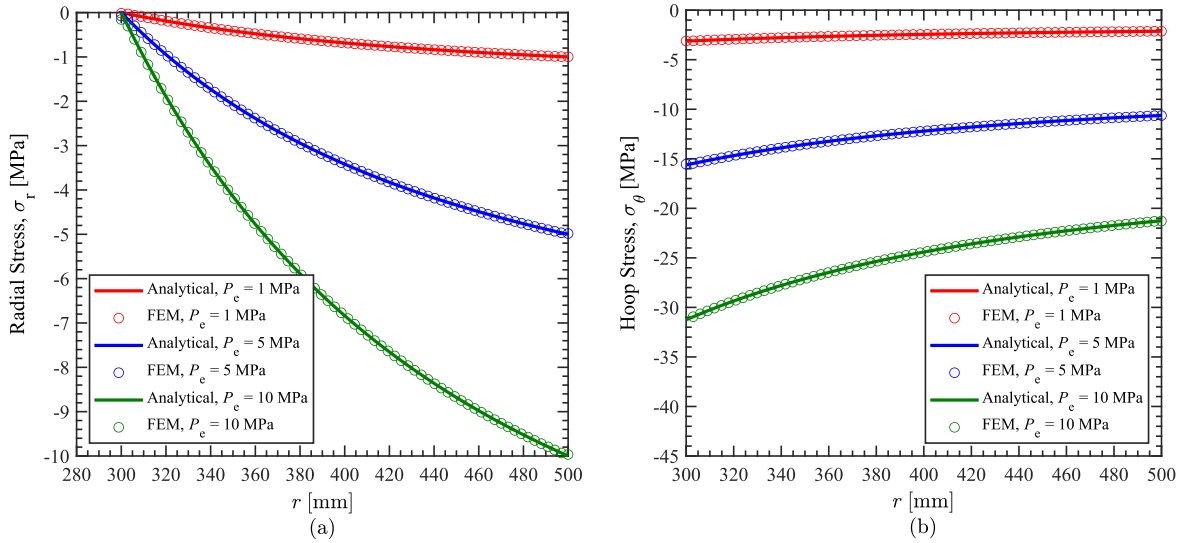

Figure 6. (a) Radial stress distribution (b) hoop stress distribution at internal pressure, P_e = 1, 5 & 10 MPa and angular velocity, ω = 0

4.3 Varying internal and external pressure without rotation for isotropic cylinder

The radial and hoop stress distributions in the isotropic thick cylinder at internal pressure, P_i = 5, 15 & 25 MPa with corresponding external pressure, P_e = 1, 5 & 10 MPa and angular velocity, ω = 0 are illustrated in Figure 7 (a) & (b). The results of Analytical Model are validated with the results of FEA as shown in Figure 7.

As depicted in Figure 7(a) the magnitude of radial stress at the deformed inner radius is equal to the applied internal pressure. The radial stress increases exponentially to reach the applied external pressure at the deformed outer radius. Figure 7(b) shows the exponential decrease in the hoop stress from the maximum value at the deformed inner radius to the minimum value at the deformed outer radius.

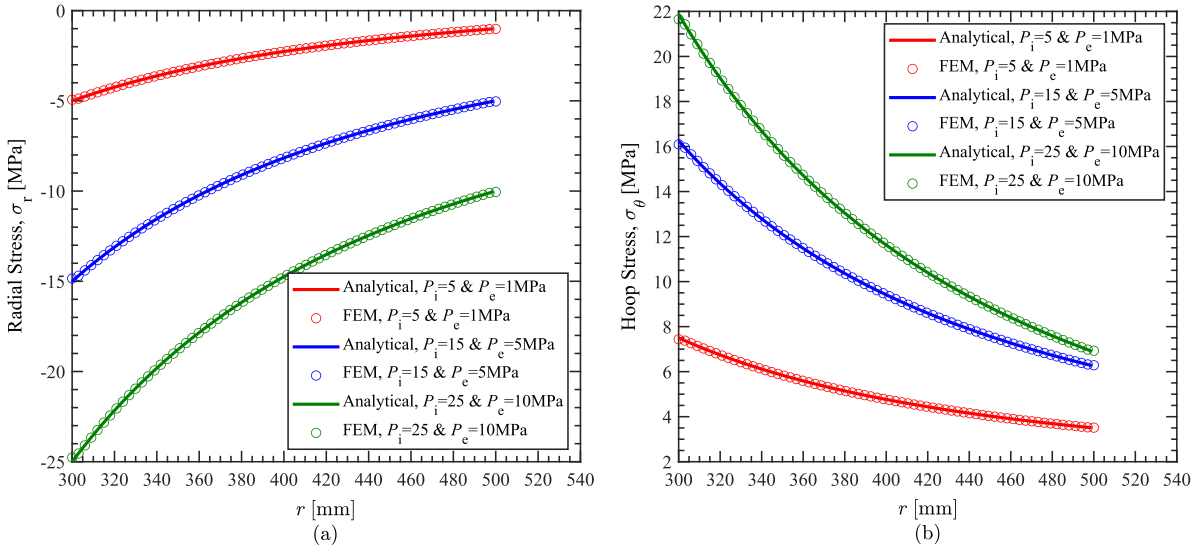

Figure 7. (a) Radial stress distribution (b) hoop stress distribution at internal pressure, P_i = 5, 15 & 25 MPa with corresponding external pressure, P_e = 1, 5 & 10 MPa

4.4 Varying angular velocity with internal pressure for isotropic cylinder

The radial and hoop stress distributions in the isotropic thick cylinder at internal pressure, P_i = 15 MPa and angular velocity, ω = 0, 1 & 2 rad/s are illustrated in Figure 8 (a) & (b). The results of Analytical Model are validated with the results of FEA as shown in Figure 8.

As depicted in Figure 8(a) the magnitude of radial stress at the deformed inner radius is equal to the applied internal pressure. The radial stress increases exponentially to reach 0 at the deformed outer radius. There is a very minor variation in the radial stresses with the increase in angular velocity. Figure 8(b) shows the exponential decrease in the hoop stress from the maximum value at the deformed inner radius to the minimum value at the deformed outer radius. There is visible increase in the hoop stress with the increase in angular velocity.

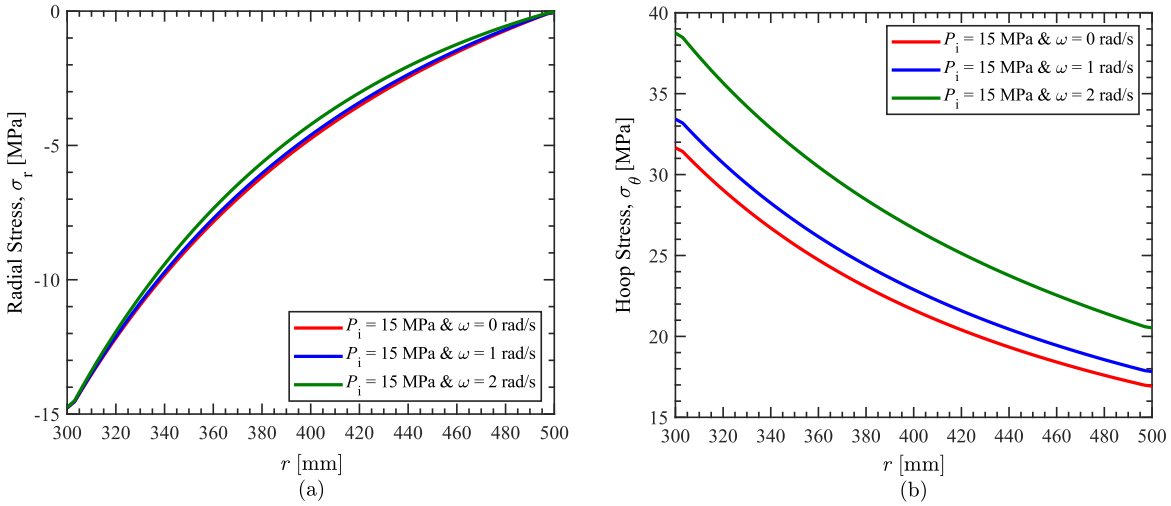

Figure 8. (a) Radial stress distribution (b) hoop stress distribution at angular velocity, ω = 0, 1 & 2 rad/s with internal pressure, P_i = 15 MPa

4.5 Comparing the functions defining Functionally Graded Materials

Carrying out the FEA for the same load conditions, the functionally graded material defined by power and exponential function is compared with the isotropic material. For an internal pressure, P_i = 0.05 MPa the different material definitions behave as shown in Figure 9.

It is evident from the results shown in Figure 9 that exponential function is the best suited for manufacturing thick cylinders as it drastically reduces the hoop stress distribution thereby, making the cylinder capable of withstanding higher pressure as compared to isotropic and power function FGM cylinder of the same dimension. Thus, the exponential function is selected for the further study of FGM thick cylinders.

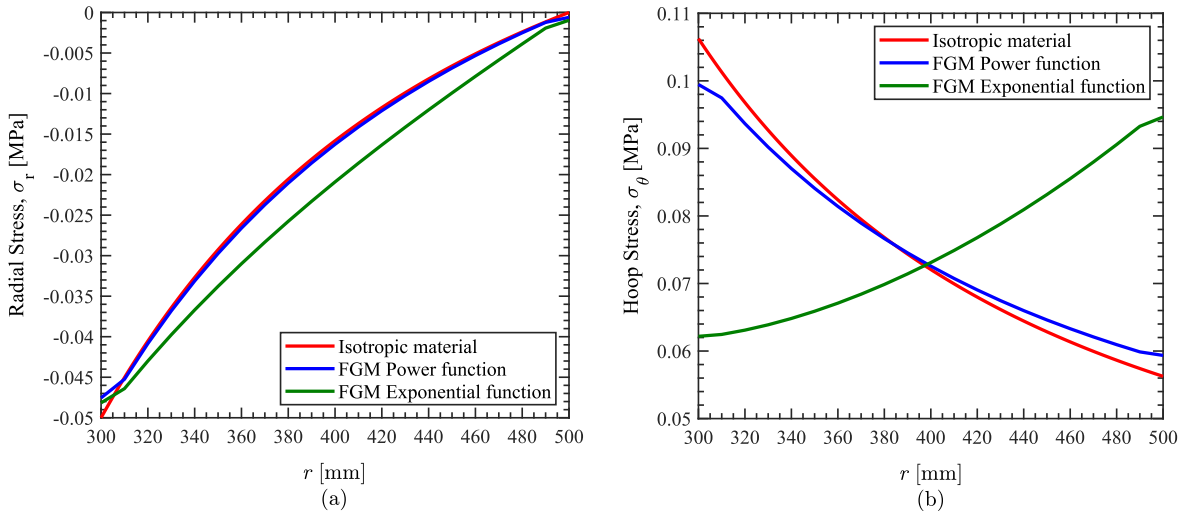

Figure 9. (a) Radial stress distribution (b) hoop stress distribution for isotropic and FGM cylinder defined by the power and exponential function at internal pressure, P_i = 0.05 MPa

4.6 Varying internal pressure without rotation for FGM cylinder

The radial and hoop stress distributions in the FGM thick cylinder defined by the exponential function at internal pressure, P_i = 5, 15 & 25 MPa and angular velocity, ω = 0 are illustrated in Figure 10 (a) & (b). The results of FEA are shown in Figure 10.

As depicted in Figure 10(a) the magnitude of radial stress at the deformed inner radius is equal to the applied internal pressure. The radial stress increases exponentially to reach 0 at the deformed outer radius. Figure 10(b) shows the increase in the hoop stress from the minimum value at the deformed inner radius to the maximum value at the deformed outer radius.

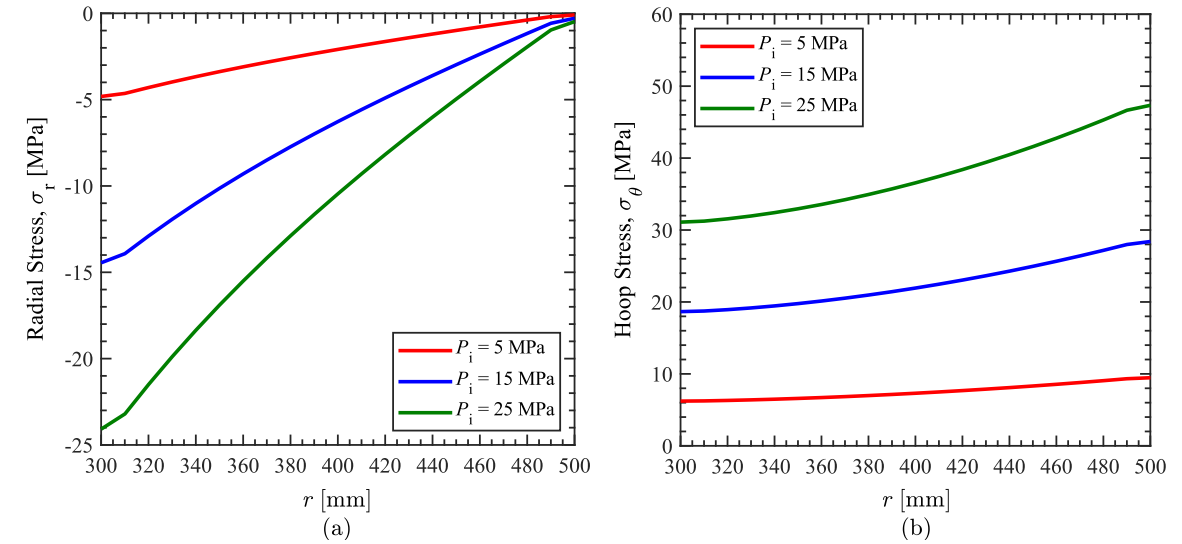

Figure 10. (a) Radial stress distribution (b) hoop stress distribution in FGM cylinder defined by the exponential function at internal pressure, P_i = 5, 15 & 25 MPa

4.7 Varying external pressure without rotation for FGM cylinder

The radial and hoop stress distributions in the FGM thick cylinder at external pressure, P_e = 1, 5 & 10 MPa and angular velocity, ω = 0 are illustrated in Figure 11 (a) & (b). The results of FEA are shown in Figure 11.

As depicted in Figure 11(a) the magnitude of radial stress at the deformed inner radius is equal to 0. The radial stress decreases exponentially to reach the applied internal pressure at the deformed outer radius. Figure 11(b) shows the exponential decrease in the hoop stress from the maximum value at the deformed inner radius to the minimum value at the deformed outer radius.

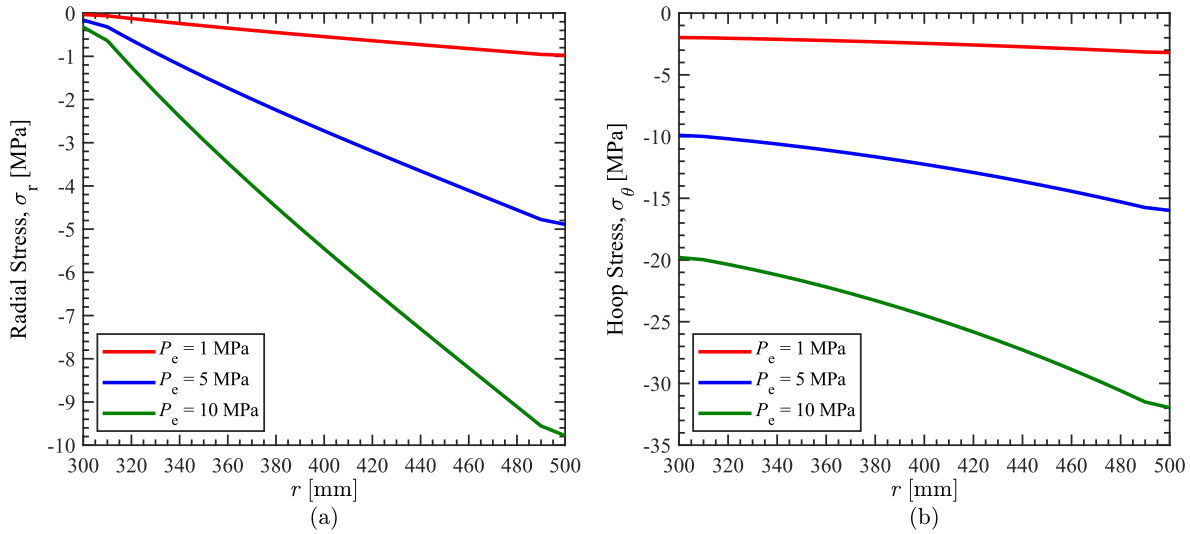

Figure 11. (a) Radial stress distribution (b) hoop stress distribution in FGM cylinder defined by the exponential function at external pressure, P_e = 1, 5 & 10 MPa

4.8 Varying internal and external pressure without rotation for FGM cylinder

The radial and hoop stress distributions in the FGM thick cylinder at internal pressure, P_i = 5, 15 & 25 MPa with corresponding external pressure, P_e = 1, 5 & 10 MPa and angular velocity, ω = 0 are illustrated in Figure 12 (a) & (b). The results of FEA are shown in Figure 12.

As depicted in Figure 12(a) the magnitude of radial stress at the deformed inner radius is equal to the applied internal pressure. The radial stress increases exponentially to reach the applied external pressure at the deformed outer radius. Figure 12(b) shows the exponential increase in the hoop stress from the minimum value at the deformed inner radius to the maximum value at the deformed outer radius.

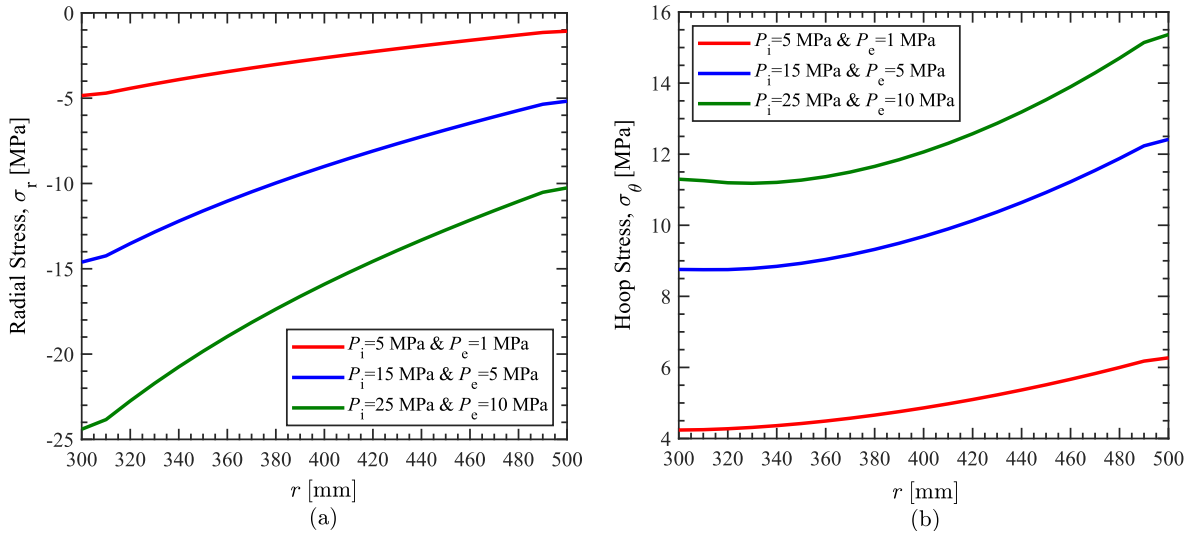

Figure 12. (a) Radial stress distribution (b) hoop stress distribution in FGM cylinder defined by the exponential function at internal pressure, P_i = 5, 15 & 25 MPa with corresponding external pressure, P_e = 1, 5 & 10 MPa

4.9 Varying angular velocity with internal pressure for FGM cylinder

The radial and hoop stress distributions in the FGM thick cylinder at internal pressure, P_i = 15 MPa and angular velocity, ω = 0, 1 & 2 rad/s are illustrated in Figure 13 (a) & (b). The results of FEA are shown in Figure 13.

As depicted in Figure 13(a) the magnitude of radial stress at the deformed inner radius is equal to the applied internal pressure. The radial stress increases exponentially to reach 0 at the deformed outer radius. There is a very minor variation in the radial stresses with the increase in angular velocity. Figure 13(b) shows the exponential increase in the hoop stress from the minimum value at the deformed inner radius to the maximum value at the deformed outer radius. There is visible increase in the hoop stress with the increase in angular velocity.

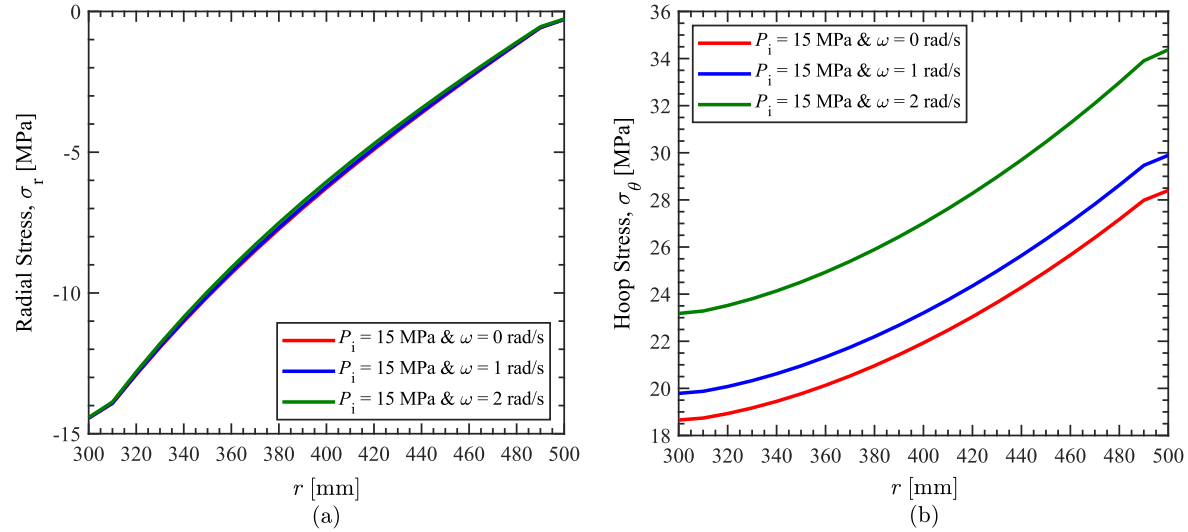

Figure 13. (a) Radial stress distribution (b) hoop stress distribution in FGM cylinder defined by the exponential function at angular velocity, ω = 0, 1 & 2 rad/s with internal pressure, P_i = 15 MPa

Chapter 5
Conclusions and Future Study

5.1 Conclusion

Isotropic and Functionally Graded cylinders behave differently under the same load and boundary conditions. The stress patterns in the FGM cylinders defined by exponential functions are completely different from that of isotropic cylinders.

The Von Misses, Radial and Hoop stress patterns obtained from FEA of Isotropic cylinder are shown in Figure 14. Similarly, the Von Misses, Radial and Hoop stress patterns obtained from FEA of FGM cylinder are shown in Figure 15.

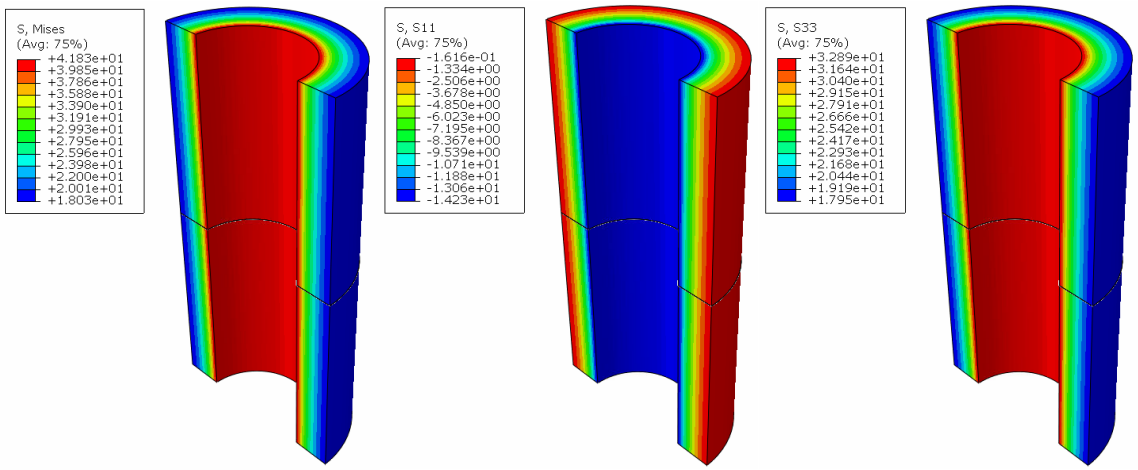

Figure 14. Isotropic Cylinder – Von Misses, Radial (S11) and Hoop (S33) stress

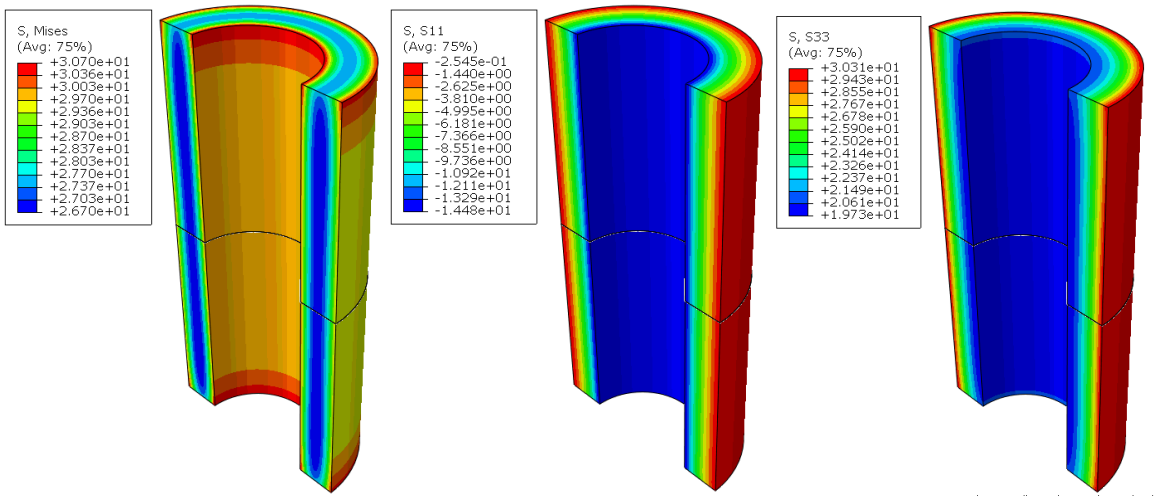

Figure 15. FGM Cylinder – Von Misses, Radial (S11) and Hoop (S33) stress

From this study, it is concluded that functionally graded materials can drastically improve the material properties as compared to isotropic materials and thus have possible applications in all major engineering fields such as aerospace, manufacturing, defence, biomedical engineering, etc. The study of these materials under possible applications in different fields is necessary to fast track the use of FGM in manufacturing the part which need better stress tolerance and longer life-cycle.

The use of functionally graded materials in hot rolling is absent from literature and industry, it is much needed to improve the manufacturing process. The present study is a preliminary study to build-up the knowledge and experience required to solve this problem.

5.2 Future Study

Finite-Element Analysis of Functionally Graded Thick Cylinder under Pressure and Rotation is the basis for the future study – **Analytical and Finite Element Modelling of FGM Roller during Hot Rolling**.

Considering the effect of hot rolling on the roller, the complete process can be approximated to a thick cylinder with internal pressure and a rotating heat flux on the external surface. As a result of high stress generated on the surface, rollers made of isotropic material are prone to erosion and deformation. This problem can be solved with the use of Functionally Graded Materials as they reduce the stresses generated on the surface of rollers.

The addition of a rotating heat flux to the FEA of FGM cylinder under pressure and rotation, will complete the FEA of FGM rollers used in hot rolling. The analytical model for FGM cylinder with a rotating heat flux is absent from the literature present till date. Future study will involve the solution of this analytical model to be validated with the results of FEA.

Results of this study will help in designing efficient rollers with better precision and longer life-cycle, reducing the manufacturing cost and improving the quality of parts manufactured.

References

[1] Zhang Wei, Feng Zhiqing, Cao Dongxing. Nonlinear dynamics analysis of aero engine blades, Journal of Dynamics and Control, 2012, 10 (3): 213 – 221.

[2] P. Zhao, S.B. Guo, G.H. Liu, Y.X. Chen, J.T. Li. Fast fabrication of W–Cu functionally graded material by high-gravity combustion synthesis and melt-in- filtration [J]. Nuclear Materials, 2014, 445: 26 - 29.

[3] J.R. Cho, H.J. Park, High strength FGM cutting tools: finite element analysis on thermo-elastic characteristics, J. Mater. Process. Technol. 130–131 (2002) 351–356.

[4] M. Afsar, J. Go, Finite element analysis of thermoelastic field in a rotating FGM circular disk, Appl. Math. Mod., 34 (2010), 3309-3320.

[5] Wang Baochen. Electromagnetic centrifugal casting of ceramic particle reinforced aluminum matrix composites [D]. 2005.

[6] G.Udupal, S. S. Rao, and K. V. Gangadharan, "Future applications of Carbon Nanotube reinforced Functionally Graded Composite Materials," in Proc. IEEE-International Conference on Advances in Engineering, Science and Management (ICAESM - 2012),March30-31,2012.

[7] Huang Rukai. Optimization design and research progress of functionally graded thermoelectric materials [J]. Journal of Chifeng University (NATURAL SCIENCE EDITION), 2016, 32 (24): 33 – 34.

[8] Neeraj Kumar and Sharma Manish Bhandari, Applications of Functionally Graded Materials (FGMs) International Journal of Engineering Research & Technology (IJERT) IJERT ISSN: 2278-0181.

[9] Naki Tutuncu, Stresses in thick-walled FGM cylinders with exponentially-varying properties, Engineering Structures 29 (2007) 2032–2035.

[10] Horgan CO, Chan AM. The pressurized hollow cylinder or disk problem for functionally graded isotropic linearly elastic materials. Journal of Elasticity 1999;55:43–59.

[11] Tutuncu, N.; Ozturk, M. 2001. Exact solutions for stresses in functionally graded pressure vessels, Composites Part B-Engineering 32(8): 683-686.

[12] Chen, Y.Z.; Lin, X.Y. 2008. Elastic analysis for thick cylinders and spherical pressure vessels made of functionally graded materials, Computational Materials Science 44(2): 581-587.

[13] Celal Evci and Müfit Gülgeç, Functionally graded hollow cylinder under pressure and thermal loading: Effect of material parameters on stress and temperature distributions, International Journal of Engineering Science 123 (2018) 92-108.

[14] Mohammad Zamani Nejad and Gholam Hosein Rahimi Elastic analysis of FGM rotating cylindrical pressure vessels, Journal of the Chinese Institute of Engineers, Vol. 33, No. 4, pp. 525-530 (2010)

[15] J.N. Sharma, Dinkar Sharma and , Sheo Kumar Stress and strain analysis of rotating FGM thermo-elastic circular disk by using FEM, International Journal of Pure and Applied Mathematics Volume 74 No. 3 2012, 339-352.

[16] G.L. Nigh, M.D. Olson, Finite element analysis of rotating disks, J. Sound Vib., 77 (1981), 61-78.

[17] Zafarmand H. Hassani B (2014) Analysis of two-dimensional functionally graded rotating thick disks with variable thickness. Acta Mech 225: 453–464.

[18] M. Zenkour, Stress distribution in rotating composite structures of functionally graded solid disks, J. Mater. Process. Technol., 209 (2009), 3511- 3517.

[19] Bayat M, Saleem M, Sahari BB, Hamouda AMS, Mahdi E (2009) Mechanical and thermal stresses in a functionally graded rotating disk with variable thickness due to radially symmetry loads. International Journal of Pressure Vessels and Piping -86: 357-372.

[20] Bayat M, Sahari BB, Saleem M, Dezvareh E. Mohazzab AH (2011) Analysis of Functionally Graded Rotating Disks with Parabolic Concave Thickness Applying an Exponential Function and the Mori-Tanaka Scheme. IOP Conf. Series: Materials Science and Engineering 17: 1-11.

[21] Rosyid A, Saheb ME, Yahia FB (2014), Stress Analysis of Nonhomogeneous Rotating Disc with Arbitrarily Variable Thickness Using Finite Element Method. Research Journal of Applied Sciences, Engineering and Technology 7: 3114-3125.

[22] S. Dewangan, L. Sondhi and Jeetendra Kumar Tiwari, Finite Element Analysis of Two Dimensional Functionally Graded Thick Rotating Disks, Int. Journal of Engineering Research and Application ISSN: 2248-9622, Vol. 7, Issue 4. (Part - 4) April 2017, pp. 91-96.

[23] *Module 9 Thin and Thick Cylinders*, ME IIT Kharagpur, NPTEL
https://nptel.ac.in/content/storage2/courses/112105125/pdf/module-9%20lesson-2.pdf

[24] Almasi, A., Baghani, M. and Moallemi, A., 2017. Thermomechanical analysis of hyperelastic thick-walled cylindrical pressure vessels, analytical solutions and FEM. International Journal of Mechanical Sciences, 130, pp.426-436.

[25] R. Hibbeler, Mechanics of materials ninth edition (2014)

Appendix

A.1 MATLAB code to plot the graphs for Isotropic cylinder

The following MATLAB code was used for validating the results of analytical model with the results of finite-element model during the parametric study of the isotropic cylinder under pressure and rotation.

```
%%%%%%%%%% Analytical Solution of Isotropic Cylinder under Pressure %%%%%%%%%%
%%%%%%%%%%%%%%%%%%%% Geometry and Load %%%%%%%%%%%%%%%%%%%%
a = 300;            % Initial Internal Radius
b = 500;            % Initial Outer Radius
qa = 25;            % Internal Pressure
qb = 10;            % External Pressure
u = 300.091;        % Deformed Internal Radius (Extracted from FEM)
v = 500.07;         % Deformed Outer Radius (Extracted from FEM)
%%%%%%%%%%%%%%%%%%%%%%%%%%%%%%%%%%%%%%%%%%%%%%%%%%%%%%%%%%%
%%%%% Calculating Radial Stress from Analytical Model %%%%%
v_isig_r = zeros(200,1);     % Pre-allocation of memory
i=1;
for r = u:1:v
isig_r = (qa*(a^2)-qb*(b^2))/((b^2)-(a^2))+...
    (((a^2)*(b^2)*(qb-qa))/((b^2)-(a^2)))*(1/(r^2));
v_isig_r(i,1) = isig_r;
i=i+1;
end
%%%%%%%%%%%%%%%%%%%%%%%%%%%%%%%%%%%%%%%%%%%%%%%%%%%%%%%%%%%
%%%%%% Calculating Hoop Stress from Analytical Model %%%%%%
v_isig_t = zeros(200,1);     % Pre-allocation of memory
i=1;
for r = u:1:v
isig_t = (qa*(a^2)-qb*(b^2))/((b^2)-(a^2))-...
    (((a^2)*(b^2)*(qb-qa))/((b^2)-(a^2)))*(1/(r^2));
v_isig_t(i,1) = isig_t;
i=i+1;
end
%%%%%%%%%%%%%%%%%%%%%%%%%%%%%%%%%%%%%%%%%%%%%%%%%%%%%%%%%%%
%%%%%%%%%%%%%%%%%%%%%%%%%%%%%%%%%%%%%%%%%%%%%%%%%%%%%%%%%%%%%%%%%%%%%%%%%%%%%%

%%%%%%%%%%%%%% Data from Finite Element Analysis (FEA) in ABAQUS %%%%%%%%%%%%%
radius = [];             % x-coordinates on a path along x-axis
radial_stress = [];      % S11 values along the same path
hoop_stress = [];        % S33 values along the same path
%%%%%%%%%%%%%%%%%%%%%%%%%%%%%%%%%%%%%%%%%%%%%%%%%%%%%%%%%%%%%%%%%%%%%%%%%%%%%%

%%%%%%%%%%%%%%%%% Plotting graphs for validation of results %%%%%%%%%%%%%%%%%%
%%%%% Vector Transformation to make the size of vectors equal %%%%%
r = u:1:v;
r = r';
```

```
%%%%%%%%%%%%%%%%%%%%%%%%%%%%%%%%%%%%%%%%%%%%%%%%%%%%%%%%%%%%%%%%%%%%%%%%%%%%
subplot(1,2,1)
plot(r,v_isig_r)
hold on
plot(r,v_isig_r)
hold on
xlabel('$\textit{r}$', 'FontName', 'Times New Roman', ...
       'FontSize',14,'Color','k', 'Interpreter', 'LaTeX')
ylabel('Radial Stress, \sigma_{r} [MPa]', 'FontName', 'Times New Roman', ...
       'FontSize',12,'Color','k')
subplot(1,2,2)
plot(r,v_isig_t)
hold on
plot(r,v_isig_t)
hold on
xlabel('$\textit{r}$', 'FontName', 'Times New Roman', ...
       'FontSize',14,'Color','k', 'Interpreter', 'LaTeX')
ylabel('Hoop Stress, \sigma_{\theta} [MPa]', 'FontName', 'Times New Roman',...
       'FontSize',12,'Color','k')
%%%%%%%%%%%%%%%%%%%%%%%%%%%%%%%%%%%%%%%%%%%%%%%%%%%%%%%%%%%%%%%%%%%%%%%%%%%%
```

A.2 MATLAB code to plot the graphs for FGM cylinder

The following MATLAB code was used for plotting the graphs for the parametric study of FGM cylinders under pressure and rotation.

```
%%%%%%%%%%%%%% Data from Finite Element Analysis (FEA) in ABAQUS %%%%%%%%%%%%
radius = [];              % x-coordinates on a path along x-axis
radial_stress = [];       % S11 values along the same path
hoop_stress = [];         % S33 values along the same path
%%%%%%%%%%%%%%%%%%%%%%%%%%%%%%%%%%%%%%%%%%%%%%%%%%%%%%%%%%%%%%%%%%%%%%%%%%%%

%%%%%%%%%%%%%%%%% Plotting graphs for validation of results %%%%%%%%%%%%%%%%%
subplot(1,2,1)
plot(radius,radial_stress,'o')
hold on
xlabel('$\textit{r}$', 'FontName', 'Times New Roman', ...
       'FontSize',14,'Color','k', 'Interpreter', 'LaTeX')
ylabel('Radial Stress, \sigma_{r} [MPa]', 'FontName', 'Times New Roman', ...
       'FontSize',12,'Color','k')
subplot(1,2,2)
plot(r,v_isig_t)
hold on
xlabel('$\textit{r}$', 'FontName', 'Times New Roman', ...
       'FontSize',14,'Color','k', 'Interpreter', 'LaTeX')
ylabel('Hoop Stress, \sigma_{\theta} [MPa]', 'FontName', 'Times New Roman',...
       'FontSize',12,'Color','k')
%%%%%%%%%%%%%%%%%%%%%%%%%%%%%%%%%%%%%%%%%%%%%%%%%%%%%%%%%%%%%%%%%%%%%%%%%%%%
```